PHARMACIA

Pharmacia 72: 1–15
DOI 10.3897/pharmacia.72.e135811

Research Article

Potential of binahong (*Anredera cordifolia* (Ten.) Steenis) leaf extract as a wound healing agent that inhibits matrix metalloproteinases (MMPs) using *in silico* and stimulates NIH-3T3 cell proliferation by *in vitro* assay

Khairunnisa Aulia Dewi[1], Susi Kusumaningrum[2], Nor Basid Adiwibawa Prasetya[1], Siska Andrina Kusumastuti[2], Eriawan Rismana[2], Ngatinem Ngatinem[3], Nuralih Nuralih[2], Mayriska Tri Wulansari[2]

1 *Diponegoro University, Semarang, Indonesia*
2 *National Research and Innovation Agency, South Tangerang, Indonesia*
3 *National Research and Innovation Research Agency, Lampung, Indonesia*

Corresponding authors: Susi Kusumaningrum (susi004@brin.go.id); Nor Basid Adiwibawa Prasetya (nor.basid.prasetya@live.undip.ac.id)

Received 29 August 2024 ♦ **Accepted** 22 November 2024 ♦ **Published** 13 February 2025

Citation: Dewi KA, Kusumaningrum S, Prasetya NBA, Kusumastuti SA, Rismana E, Ngatinem N, Nuralih N, Wulansari MT (2025) Potential of binahong (*Anredera cordifolia* (Ten.) Steenis) leaf extract as a wound healing agent that inhibits matrix metalloproteinases (MMPs) using *in silico* and stimulates NIH-3T3 cell proliferation by *in vitro* assay. Pharmacia 72: 1–15. https://doi.org/10.3897/pharmacia.72.e135811

Abstract

The wound healing process goes through a complex mechanism and takes a long time. Based on empirical experience, binahong leaves (*Anredera cordifolia* (Ten.) Steenis) heal fresh wounds. This study aims to determine the potential of binahong extract as an active ingredient for wound healing through *in silico* and *in vitro* testing. Extraction of the leaves using the ultrasonication method with several different solvents: ethyl acetate–ethanol and aqueous ethanol with a definite ratio. Based on UHPLC-HRMS analysis, the 96% ethanol extract identified 187 compounds, the 70% ethanol extract 153 compounds, the 50% ethanol extract 105 compounds, and the ethyl acetate extract 110 compounds. In silico study showed that the trans-3-indole acrylic acid compound with MMP1 produces a binding energy of -8.0 kcal/mol, while the MMP1 native ligand produces -9.5 kcal/mol. The gluconic acid compound with MMP12 produces a binding energy of -4.3 kcal/mol, while for the native ligand, MMP12 produces -3.4 kcal/mol. Both compounds were identified in *Anredera cordifolia* (Ten.) Steenis extract with a 70% ethanol solvent. An in vitro assay was conducted using a fibroblast cell proliferation assay over 24, 48, and 72 hours using the MTT method. Extract with 70% ethanol in the 24-hour incubation period significantly increased cell proliferation, but in the 48- and 72-hour incubation periods, it tended to be stable. 70% ethanol of *Anredera cordifolia* (Ten.) Steenis at 8 µg/mL–200 µg/mL concentrations can significantly increase cell proliferation compared to extracts with other solvents. These results indicate that the 70% ethanol extract of *Anredera cordifolia* (Ten.) Steenis has the best activity to accelerate the proliferation process, which can be the initial step to repair the wound. This study revealed that 70% ethanol of *Anredera cordifolia* (Ten.) Steenis is potent as a wound-healing agent.

Keywords

Anredera cordifolia (Ten.) Steenis leaves, wound healing, molecular docking, matrix metalloproteinases, in vitro

Introduction

The skin is an essential natural barrier that protects internal organs from environmental elements that might lead to sores. (Wang et al. 2021). Healing a wound involves several intricate steps, such as hemostasis, inflammation, proliferation, and remodeling (Zhao et al. 2020). This process begins with the occurrence of an injury and may continue for months or even years. Several factors can cause prolonged wound healing, such as impaired growth factor production, chronic inflammation, and impaired angiogenesis (Mohammadi et al. 2019; Rehman et al. 2019).

Matrix metalloproteinases (MMPs) are endopeptidases involved in all stages of wound healing. MMPs cause the capillary basement membrane to rupture during the proliferation stage, which promotes cell migration and angiogenesis. On the other hand, during the tissue remodeling stage, MMP activity decreases and induces the release of growth factors for remodeling (Ke et al. 2021). During angiogenesis, MMP1 is a significant collagenase expressed at the wound site. It causes a decrease in type 1 collagen, an essential dermal component that promotes keratinocyte migration and epidermal regeneration during wound healing. MMP1 is automatically inhibited throughout the remodeling process and remains active until the wound is closed. However, excessively high levels of MMPs correlate with chronic wounds and will lead to longer healing times (Arda et al. 2024). A metalloelastase called MMP12 also contributes significantly to wound healing by disrupting the extracellular elastin matrix, allowing immune cell invasion, and contributing to inflammation and granuloma formation.

Some studies have observed a shift from traditional allopathic treatments towards the integration of herbal plants, aiming to hasten the healing of wounds (Moraes et al. 2011). *Anredera cordifolia* (Ten.) Steenis (ACS), commonly known as Binahong, is a medicinal plant in the Basellaceae family. Herbal treatments can be made from parts of the ACS plant, such as its leaves, stems, and tubers (Astuti et al. 2011). ACS extract stimulates fibroblast formation and collagen production, accelerating wound healing (Yuliani et al. 2012; Yuniarti and Lukiswanto 2017). The process is significantly aided by the secondary metabolites found in ACS leaf extract, including saponins, terpenoids, flavonoids, tannins, alkaloids, triterpenes, anthraquinones, glycosides, steroids, and phenolic acids (Salasanti et al. 2014; Khoswanto and Soehardjo 2018; Hanafiah et al. 2021). The flavonoids found are apigenin, quercetin, apigetrin, vitexin, rutin, myricetin, and morin (Sukandar et al. 2016; Leliqia et al. 2017; Mulia et al. 2017). Besides, the phenolic acids in ACS leaf extract are p-coumaric acid, and the triterpenes found are oleanolic acid and ursolic acid (Leliqia et al. 2017; Fachriyah et al. 2019). Previous studies on compounds successfully isolated in ACS extract are very limited. One of them is 3-hydroxy-alpha-ionone, which has allelopathic activity (Bari et al. 2019). Other compounds isolated from ACS leaf extracts include 3,5,3',4'-tetrahydroxyflavone and the flavonoid 8-glucopyranosyl-4',5,7-trihydroxyflavone, or vitexin. Vitexin exhibited antioxidant activity when tested with the 2,2-diphenyl-1-picrylhydrazyl (DPPH) method and demonstrated in vitro α-glucosidase inhibitory activity and antidiabetic activity in alloxan-induced mice (Alba et al. 2020). Previous research showed that 19 compounds in hexane extract were identified using GC-MS. ACS 70 extract contained phytol (35.68%), cis-cis, cis-7,10,13-hexadecatrienal (9.94%), 2,3-dihydroxy propyl palmitate (6, 6, and 27%), 2-ethyl butyric acid, monododecyl ester (5.86%), and hexadecanoic acid (1.61%–5.12%). The result also identified the presence of squalene, hexadecanoic acid, methyl ester, 3 (2H)-selenophene, 2-(dihydro-4,4-dimethyl-3-oxo selenophene-2 (3H)–ylidene-0-dihydro 4,4-dimethyl, neophytadiene, and 9-octadecanoid acid with a smaller percentage than other ingredients (Feriyani et al. 2020). The volatile constituents of the ACS plant were analyzed, and the major compounds were phytol (15.33%), alpha-pinene (9.0%), and 6,10,14-trimethyl pentadecanone (6.12%). Numerous research works have documented the efficiency of ACS extracts in wound healing. For instance, the ethanol fraction from its leaves has been shown to promote fibroblast proliferation (Hanafiah et al. 2019). Another study found that ACS leaf extract in gel form is effective in treating diabetic wounds in rats (Kintoko and Desmayanti 2016), and both topical and oral administration of the extract have been shown to improve diabetic wounds (Anggraeni et al. 2017).

This study aims to identify compounds in ACS extracts obtained from different solvents – ethyl acetate (ACS EA), 96% ethanol (ACS 96), 70% ethanol (ACS 70), and 50% ethanol (ACS 50) – that may serve as effective wound healing agents. The compounds in the ACS extracts were identified using UHPLC-HRMS, followed by molecular docking to predict their interactions with MMP1 and MMP12. The wound healing potential was evaluated by testing the ACS extracts on NIH-3T3 fibroblast cell proliferation. The study identified compounds from the ACS extract with the potential to inhibit MMP1 and MMP12, which have also been shown to stimulate fibroblast cell proliferation, thereby promoting wound healing.

Materials and methods

Materials and instruments

The study utilized a Windows 10 laptop equipped with 8.00 GB RAM and an Intel Core i7 processor, alongside software including ChemDraw 22.2.0, Chem3D 22.2.0, BIOVIA Discovery Studio Visualizer 2021, PyRx 0.9.9, and AutoDock Tools 1.5.7. Additional materials included ethanol, ethyl acetate, distilled water, and an ultrasonicator (Powersonic 410). MMP1 (PDB ID: 996C) and MMP12 (PDB ID: 1Y93) were used for the molecular docking study, and their structures were obtained from https://www.rcsb.org/. The three-dimensional structure of the test ligand ACS extract compound was downloaded from https://pubchem.ncbi.nlm.nih.gov/.

Plant material

The material used was dried *Anredera cordifolia* (Ten.) Steenis, sourced from the medicinal plant experimental garden Research Center for Pharmaceutical Ingredients and Traditional Medicine, the National Research and Innovation Agency Badan Riset dan Inovasi Nasional of Indonesia (BRIN) Anak Tuha, Sulusuban in Lampung Province, Sumatra, Indonesia, in 2022 (Fig. 1). The botanical material was collected by Sri Ningsih from the Research Center for Pharmaceutical Ingredients and Traditional Medicine, the National Research and Innovation Agency, and identified by Arifin Surya Dwipa Irsyam, Curator Herbarium from the School of Life Sciences and Technology, Bandung Institute of Technology, with determination result report No. 7841/IT1.C11.2/TA.00/2023. Herbarium specimen is a collection of PRBBOOT, with the code PRBBOOT_007_2022.

Extraction of *Anredera cordifolia* (Ten.) Steenis

The plant leaves were oven dried at 40 °C until constant weight was reached, and they were powdered using an electric grinder. To prepare the crude extracts for UH-PLC-HRMS analysis and in vitro assay, dry powder leaves were dissolved in 96% ethanol (ACS 96), 70% ethanol (ACS 70), 50% ethanol (ACS 50), and ethyl acetate (ACS EA) at a ratio of 1:40 and left on ultrasonic apparatus at room temperature for 30 minutes. The extracts were then filtered using a paper filter, and the supernatant was transferred using the same procedure. The supernatant was transferred using the same evaporator flask. The supernatant was then concentrated using a rotary vacuum evaporator at 50 °C and dried using freeze-drying to obtain dry extracts.

Figure 1. *In situ* photo of *Anredera cordifolia* (Ten.) Steenis. Photo by Ngatinem in the medicinal plant experimental garden Research Center for Pharmaceutical Ingredients and Traditional Medicine, the National Research and Innovation Agency (BRIN), Anak Tuha, Sulsuban in Lampung Province, Sumatra, Indonesia.

Analysis of *Anredera cordifolia* (Ten.) Steenis extract using UHPLC-HRMS

For UHPLC-HRMS analysis, samples were prepared by rotary evaporator and freeze-dried 200 mL of each extract until dry. 10 mg extract was reconstituted in 2 mL methanol, then ultrasonicated and filtered using Syringe Filter Regenerated Cellulose (RC) poresize 0.2 um diameter 25 mm before being transferred into MS vials. The analysis was conducted using ultra-high-pressure liquid chromatography combined with Orbitrap high-resolution mass spectrometry, the Thermo Scientific™ Vanquish™ UHPLC Binary Pump, and the Thermo Scientific™ Q Exactive™ Hybrid Quadrupole-Orbitrap™ High-Resolution Mass Spectrometer. The liquid chromatography utilized a Thermo Scientific™ Accucore™ Phenyl-Hexyl 100mm × 2.1mm ID × 2.6µm analytical column. The method followed was based on Windarsih et al. (2022), with mobile phases consisting of MS-grade water containing 0.1% formic acid (A) and MS-grade methanol containing 0.1% formic acid (B), applied using a gradient technique at a flow rate of 0.3 mL/min. The gradient started with 5% of mobile phase B, gradually increasing to 90% over 16 minutes, held at 90% for 4 minutes, and then returned to the initial condition (5% B) by the 25-minute mark. The column temperature was maintained at 40 °C, with an injection volume of 3 µL. The non-target screening was conducted in full MS/dd-MS2 acquisition mode with a positive or negative polarity or ionization state. The arbitrary units (AU) for nitrogen were 32, 8, and 4, and it was utilized as a sheath, auxiliary, and purge gas. The auxiliary gas heater temperature was adjusted to 30 °C, the capillary temperature to 320 °C, and the spray voltage to 3.30 kV. With a resolution of 70,000 for full MS and 17,500 for dd-MS2 in both positive and negative ionization modes, the scanning range was 66.7 to 1000 m/z. The system was operated via Thermo Scientific, Bremen, Germany's XCalibur 4.4 software. To maintain the best possible instrument performance and resilience in mass accuracy-related studies, the device was calibrated once a week in both positive and negative ESI modes using Thermo Scientific Pierce ESI ion calibration solution (Waltham, MA).

Molecular docking study

Preparation of ligands and proteins for molecular docking

The macromolecular structures of MMP1 (PDB ID: 996C) and MMP12 (PDB ID: 1Y93) proteins and their native ligands for molecular docking were taken from the Protein Data Bank (https://www.rcsb.org/). BIOVIA Discovery Studio Visualizer 2021 software obtained protein structures purified from other components, such as water molecules and their native ligands. It is then saved as a receptor (without ligand) in PDB format. This step also separates the native ligand from the macromolecule.

The ligands used for docking simulation are ligands from protein structures (native ligands), and ACS extracts compounds from UHPLC-HRMS analysis results. The design of the ligand structure was carried out using ChemDraw 22.2.0 software. The structure was then modified by adding or deleting according to the PubChem database structure source (https://pubchem.ncbi.nlm.nih.gov) and saved in .cdx format. The 2D structure was then converted into 3D to minimize the energy (MM2) using Chem3D 22.2.0 software stored in PDB format.

Molecular docking

Grid positioning was performed by positioning the native ligand using Vina Wizard on PyRx 0.9.9 (Ayodele et al., 2023). The grid box coordinates for MMP1 were X = 8.786, Y = -10.977, and Z = 38.673, while those for MMP12 were X = 1.095, Y = -1.779, and Z = 4.740. The method was validated using PyRx 0.9.9 software through a process known as redocking, where the native ligand is rebonded to the prepared receptor protein multiple times until the binding affinity results are constant and the root mean square deviation (RMSD) value is ≤ 2 Å (Muttaqin 2019). All of the ACS-extracted chemicals from the UHPLC-HRMS analysis were docked to MMP1 and MMP12 once the validation phase was deemed qualified. BIOVIA Discovery Studio Visualizer 2021 was used to visualize 2D docking. Van der Waals interactions, charge, and hydrogen bonding were also examined, and the ligand position with the best binding energy (-ΔG, kcal/mol) was chosen.

In vitro analysis using NIH-3T3 cells

Sample preparation

We weighed dry extracts and dissolved them in DMSO to obtain 50.000 µg/L. Then, we diluted the extracts in a medium culture until we reached a specific concentration of extracts.

Cell line

We used NIH-3T3/Swiss mouse embryos from the Food and Science Technology Department of National Pingtung Science Technology (NPUST, Pingtung, Taiwan). Cells were cultured in Dulbecco's Modified Eagle's Medium (DMEM; Gibco, New York, USA) supplemented with 10% fetal bovine serum and 1% penicillin/streptomycin (PS, 100 units of penicillin/mL and 100 pg streptomycin/mL, Gibco, New York, USA) at 37 °C with 5% CO_2.

Cell viability assay

Initially, a preliminary study was carried out to establish the non-toxic concentration of the extract on NIH-3T3 fibroblast cells. Cell viability was determined using the 3-[4,5-dimethylthiazol-2-yl]-2,5-diphenyl tetrazolium bromide (MTT) method. NIH-3T3 fibroblast cells were plated at 1×10^5 cell/mL in a 96-well plate and incubated for 24 hours at 37 °C in a humidified 5% CO_2 environment (Agustini et al. 2024). The cells were incubated for 24 hours with different extract concentrations (25, 50, 100, 200, and 400 µg/mL). After removing the culture media, the cells were cleaned with phosphate buffer saline (PBS). Following a 4-hour incubation period, 100 µl of 0.5 mg/mL MTT and 100 µl of 10% SDS were applied to the cells. An ELISA

reader (Synergy HTX; Bio-Tek Instruments Inc., Winooski, VT, USA) was used to measure the cells' absorbance after being incubated for the entire night in a dark environment. Cell viability (%) = ([Abs of sample / Abs of control] ×100) was the formula used to calculate cell viability.

Cell proliferation assay

ACS extracts prepared with different solvents – 96% ethanol, 70% ethanol, 50% ethanol, and ethyl acetate – were tested for cell proliferation assay. The NIH-3T3 cell line (5×10^3 cells/mL) was cultured in DMEM complete medium for 24 hours. Extracts were introduced at various concentrations (2, 8, 40, and 200 µg/mL) and incubated for 24, 48, and 72 hours. MTT assay and cell viability were calculated to measure proliferation activity (Zihlif et al. 2013).

Statistical analysis

SPSS software was used to examine all of the grouped data. The standard deviation (SD) from three replicates is used to express the results. A t-test was used for statistical comparisons between two groups, or an independent t-test was used for comparisons between more than two groups. Statistical significance was defined as a $p > 0.05$.

Results and discussion

Analysis of *Anredera cordifolia* (Ten.) Steenis extract compounds with UHPLC-HRMS

This study used UHPLC-HRMS analysis to identify the compounds in ACS EA, ACS 96, ACS 70, and ACS 50 extracts. UHPLC-HRMS allows for the comprehensive screening of small molecules in the sample (Windarsih et al. 2022). The results of this analysis include a predicted match between the identified compounds and the m/z Cloud database. Using a high-resolution mass spectrometer, the mzCloud database houses MS and MS/MS spectra collected for various molecules. These spectra can be used as a reference when searching for unknown substances. Molecular identification is based on high-resolution data from intact molecular ions and all fragment ions. In order to assess possible matches, the Compound Discoverer program compares the recorded fragmentation patterns and molecular ion patterns with those in the m/zCloud database. If a match is found, the software assigns a score from 0 to 100, with higher scores indicating more matched ions. (Kostikova et al. 2021).

The UHPLC-HRMS results have found that in ACS 96, there are 187 compounds; in ACS 70, 153 compounds; in ACS 50, 105 compounds; and in ACS EA, 108 compounds. The compounds contained in each extract are the same, so these compounds are sorted to determine the best compounds for the wound healing process. Thirty-three compounds from different solvent variations were successfully filtered, potentially accelerating wound-healing. As shown in Table 1, each solvent variation contains some compounds, such as compounds (2), (4), and (7), which are present in ACS EA, ACS 96, ACS 70, and ACS 50 extracts, but with varying degrees of match. Compound (2) has the highest level of fit in ACS EA at 78.8% and decreases as the level of polarity in the solvent increases. In addition, certain compounds are exclusive to extracts with specific solvents. For example, compounds (5), (6), (8), (11), and (17) are only found in the ACS 96 extract, while compounds (32) and (33) are found only in the ACS EA extract. On the other hand, the compounds contained in ACS 70 and ACS 50 extracts share some similarities but differ in match numbers depending on the properties of the compound, indicating that the solvent choice significantly impacts the extracted compounds' content.Generally, secondary metabolite compounds in *Anredera cordifolia* (Ten.) Steenis leaves tend to dissolve in polar solvents. Ethanol at 96% concentration has a high filtering ability, allowing it to extract polar, non-polar, and semi-polar compounds. Meanwhile, 70% ethanol is more polar than 96% but less polar than 50%. Changes in ethanol concentration directly affect the solvent's polarity, with polarity increasing as ethanol concentration decreases in water (Riwanti et al. 2020). Semi-polar secondary metabolites are more likely to be extracted using ethyl acetate.

In Silico molecular inhibition of *Anredera cordifolia* (Ten.) Steenis leaf extract compounds against MMP1 and MMP12 activities

Among the 33 ACS extract compounds, 16 showed good binding affinity values for MMP1, 15 had high binding values for MMP12, and the remaining 2 compounds showed high binding values for both MMP1 and MMP12. The molecular interactions between the identified compounds from ACS 96, ACS 70, ACS 50, and ACS EA extracts with MMP1 and MMP12 activities are presented in Table 2. These 33 compounds, along with two native ligands, were visualized in 3D structures obtained from the PubChem database in .pdb format and processed using BIOVIA Discovery Studio Visualizer 2021 software. The native ligands of MMP1 and MMP12 were identified as n-hydroxy-2-[4-(4-phenoxy-benzenesulfonyl)-tetrahydro-pyran-4-yl]-acetamide (LN1) and acetohydroxamic acid (LN12), respectively. Notably, n-hydroxy-2-[4-(4-phenoxy-benzenesulfonyl)-tetrahydro-pyran-4-yl]-acetamide is the reference drug for MMP1, while acetohydroxamic acid is the reference drug for MMP12, which is also the protein's native ligand. These native ligands are confirmed to bind to the major active residues of each protein (Arda et al. 2024).

Among all the compounds analyzed, trans-3-indoleacrylic acid, found in the ACS 96 and ACS 70 extracts, exhibited the lowest binding affinity to MMP1 with a value of -8.0 kcal/mol. However, this binding score was still lower than that of the native ligand, which had a binding affinity of -9.5 kcal/mol for MMP1. Binding energy values of test ligands smaller than or equal to the native ligand indicate less than optimal binding stability (Nissa et al. 2022). The native ligand formed hydrogen bonds with ALA 182, ASN 180, LEU 181, VAL 215, PRO 238, and GLU 219, classified as medium to strong hydrogen bonds. The native ligand is also connected with two hydrophobic bonds, TYR 240 and ARG 214.

Table 1. LC-HRMS results of *Anredera cordifolia* (Ten.) Steenis compounds.

Extract Type	Compound (Compound Number)	Formula	MW	RT (min)	m/z Cloud Best Match (%)
ACS 96	Trans-3-indole acrylic acid (1)	$C_{11}H_9NO_2$	187,063	3.53	80,7
	6-(2-hydroxy-4-phenylbutyl)-4-methoxy pyran-2-one (2)	$C_{16}H_{18}O_4$	274,1203	9,125	72,8
	8-{3-Oxo-2-[(2E)-2-penten-1-yl]-1-cyclopenten-1-yl}octanoic acid (3)	$C_{18}H_{28}O_3$	292,2037	12,571	75,6
	(R, Z)-N-(1-hydroxy-3-phenylpropan-2-yl)benzimidic acid (4)	$C_{16}H_{17}NO_2$	255,1259	8,477	91,3
	7-Methyl-3-methylene-6-(3-oxobutyl)-3,3a,4,7,8,8a-hexahydro-2H-cyclohepta[b]furan-2-one (5)	$C_{15}H_{20}O_3$	248,141	7,381	81,9
	1a,5,7a-trimethyl-1a,6a,7a,8,9,9a-hexahydrobis(oxireno)[2',3':4,5;2",3":8,9]cyclodeca[1,2-b]furan-6(2H)-one (6)	$C_{15}H_{18}O_4$	262,1201	9,067	82,8
	12-Oxo phytodienoic acid (7)	$C_{18}H_{28}O_3$	292,2038	11,178	83,3
	Curcolonol (8)	$C_{15}H_{20}O_4$	264,1361	7,749	83,8
	5-(7-hydroxy-6-methyloctyl)furan-2(5H)-one (9)	$C_{13}H_{22}O_3$	226,1567	6,095	75
	L(-)-2-Amino-3-phenyl-1-propanol (10)	$C_9H_{13}NO$	151,0995	1,801	87,4
	L-Phenylalanine (11)	$C_9H_{11}NO_2$	165,0791	1,496	84,6
	Nicotinic acid (12)	$C_6H_5NO_2$	123,0321	1,091	93,4
	4-Phenylbutyric acid (13)	$C_{10}H_{12}O_2$	164,0834	18,204	98,8
	Azelaic acid (14)	$C_9H_{16}O_4$	188,1042	6,636	95,6
	Phthaldialdehyde (15)	$C_8H_6O_2$	134,0368	5,254	69,8
	6-Pentyl-2H-pyran-2-one (16)	$C_{10}H_{14}O_2$	166,0994	9,11	73,9
	Jasmone (17)	$C_{11}H_{16}O$	164,1202	8,391	65,6
ACS 70	Trans-3-indoleacrylic acid (1)	$C_{11}H_9NO_2$	187,0632	3,476	82,9
	6-(2-hydroxy-4-phenylbutyl)-4-methoxypyran-2-one (2)	$C_{16}H_{18}O_4$	274,1203	9,156	69,1
	8-{3-Oxo-2-[(2E)-2-penten-1-yl]-1-cyclopenten-1-yl}octanoic acid (3)	$C_{18}H_{28}O_3$	292,2036	10,688	83,1
	(R, Z)-N-(1-hydroxy-3-phenylpropan-2-yl)benzimidic acid (4)	$C_{16}H_{17}NO_2$	255,1259	8,414	91,3
	4-(5,6-dihydroxyheptyl)-3-methylfuran-2(5H)-one (18)	$C_{12}H_{20}O_4$	228,1362	8,443	65,1
	12-Oxo phytodienoic acid (7)	$C_{18}H_{28}O_3$	292,2035	9,211	84,1
	19-Norandrostenedione (19)	$C_{18}H_{24}O_2$	272,1775	10,053	69,7
	Vitexin (20)	$C_{21}H_{20}O_{10}$	432,1055	5,712	75,5
	9S,13R-12-Oxophytodienoic Acid (21)	$C_{18}H_{28}O_3$	292,2036	11,105	83,3
	7-(2-aminophenyl)heptanoic Acid 22)	$C_{13}H_{19}NO_2$	221,1415	4,822	69,8
	Gluconic acid (23)	$C_6H_{12}O_7$	196,0578	0,842	71,8
	L(-)-2-Amino-3-phenyl-1-propanol (10)	$C_9H_{13}NO$	151,0999	1,771	76,4
	L-Phenylalanine (11)	$C_9H_{11}NO_2$	165,0791	1,436	93,4
	Nicotinic acid (12)	$C_6H_5NO_2$	123,0321	1,032	93,4
	Uracil (24)	$C_4H_4N_2O_2$	112,0275	1,013	83,1
	2,4-Dimethylbenzaldehyde (25)	$C_9H_{10}O$	134,0731	10,895	70,3
	4-Phenylbutyric acid (13)	$C_{10}H_{12}O_2$	164,0834	18,136	100
	Guanine (26)	$C_5H_5N_5O$	151,0495	0,986	88,8
	Azelaic acid (14)	$C_9H_{16}O_4$	188,1043	6,573	94,9
	Hypoxanthine (27)	$C_5H_4N_4O$	136,0385	1,019	93,4
ACS 50	6-(2-hydroxy-4-phenylbutyl)-4-methoxypyran-2-one (2)	$C_{16}H_{18}O_4$	274,1204	9,127	67,4
	(R, Z)-N-(1-hydroxy-3-phenylpropan-2-yl)benzimidic acid (4)	$C_{16}H_{17}NO_2$	255,1259	8,384	92,5
	4-(5,6-dihydroxyheptyl)-3-methylfuran-2(5H)-one (18)	$C_{12}H_{20}O_4$	228,1361	8,415	65,2
	12-Oxo phytodienoic acid (7)	$C_{18}H_{28}O_3$	292,2038	8,611	88,2
	19-Norandrostenedione (19)	$C_{18}H_{24}O_2$	272,1776	10,02	67,7
	Vitexin (20)	$C_{21}H_{20}O_{10}$	432,1055	5,683	75,9
	9S,13R-12-Oxophytodienoic Acid (21)	$C_{18}H_{28}O_3$	292,2036	10,655	82,7
	Jasmonic acid (28)	$C_{12}H_{18}O_3$	210,1254	5,376	81,7
	4-Coumaric acid (29)	$C_9H_8O_3$	164,0474	5,356	75,6
	Corchorifatty acid F (30)	$C_{18}H_{32}O_5$	382,2249	8,608	82,5
	Gluconic acid (23)	$C_6H_{12}O_7$	196,0579	0,808	98,4
	Nicotinic acid (12)	$C_6H_5NO_2$	123,0321	1,004	93,4
	Uracil (24)	$C_4H_4N_2O_2$	112,0274	0,987	81,5
	Guanine (26)	$C_5H_5N_5O$	151,0494	0,963	96,5
	Azelaic acid (14)	$C_9H_{16}O_4$	188,1042	6,544	93,8
	Hypoxanthine (27)	$C_5H_4N_4O$	136,0385	0,996	93,1
	Phthaldialdehyde (15)	$C_8H_6O_2$	134,0368	5,738	76
	Citric acid (31)	$C_6H_8O_7$	192,0262	0,973	95,5

Extract Type	Compound (Compound Number)	Formula	MW	RT (min)	m/z Cloud Best Match (%)
ACS EA	6-(2-hydroxy-4-phenylbutyl)-4-methoxypyran-2-one (2)	$C_{16}H_{18}O_4$	274,1204	9,128	78,8
	8-{3-Oxo-2-[(2E)-2-penten-1-yl]-1-cyclopenten-1-yl}octanoic acid (3)	$C_{18}H_{28}O_3$	292,2038	11,066	83,3
	(R, Z)-N-(1-hydroxy-3-phenylpropan-2-yl)benzimidic acid (4)	$C_{16}H_{17}NO_2$	255,126	8,388	91,6
	(9cis)-Retinal (32)	$C_{20}H_{28}O$	284,2141	15,413	71,3
	12-Oxo phytodienoic acid (7)	$C_{18}H_{28}O_3$	292,2038	8,626	82,9
	19-Norandrostenedione (19)	$C_{18}H_{24}O_2$	272,1778	14,29	78,8
	9S,13R-12-Oxophytodienoic Acid (21)	$C_{18}H_{28}O_3$	292,2038	21,54	74,9
	Corchorifatty acid F (30)	$C_{18}H_{32}O_5$	328,225	8,614	81,4
	2,4-Dimethylbenzaldehyde (25)	$C_9H_{10}O$	134,0732	10,888	74,3
	4-Phenylbutyric acid (13)	$C_{10}H_{12}O_2$	164,0834	18,118	97,2
	Phthaldialdehyde (15)	$C_8H_6O_2$	134,0368	5,734	62,5
	6-Pentyl-2H-pyran-2-one (16)	$C_{10}H_{14}O_2$	166,0995	9,017	67,6
	(R, Z)-N-(1-hydroxy-3-phenylpropan-2-yl)acetamide acid (33)	$C_{11}H_{15}NO_2$	193,1099	11,743	81,4

Table 2. Interaction of *Anredera cordifolia* (Ten.) Steenis compounds and reference compounds in the active site of MMP1 and MMP12.

Extract Type	Compound (Compound number)	Bond interaction	Amino acid residue	Bond energy (kcal/mol)
		MMP1		
Native ligand	n-hydroxy-2-[4-(4-phenoxy-benzenesulfonyl)-tetrahydro-pyran-4-yl]-acetamide (LN1)	Hydrogen bond	LEU 181, ASN 180, ALA 182, VAL 215, PRO 238, GLU 219	-9.5
		Hydrophobic bond	TYR 240, ARG 214	
		Van der Waals	THR 241, SER 239, LEU 235, TYR 237, HIS 218, HIS 183, HIS 222, HIS 228, GLY 179	
ACS 96	Trans-3-indoleacrylic acid (1)	Hydrogen bond	TYR 237, ALA 182	-8.0
		Hydrophobic bond	VAL 215, HIS 218, SER 239	
		Van der Waals	LEU 235, THR 241, ARG 214, TYR 240, LEU 181, GLY 179, ASN 180, PRO 238	
	6-(2-hydroxy-4-phenylbutyl)-4-methoxypyran-2-one (2)	Hydrogen bond	ALA 182, ASN 180, HIS 183	-7.8
		Hydrophobic bond	HIS 218, SER 239, HIS 228, VAL 215	
		Van der Waals	TYR 237, LEU 235, THR 241, ARG 214, TYR 240, LEU 181, ALA 184, GLU 219, HIS 222	
	8-{3-Oxo-2-[(2E)-2-penten-1-yl]-1-cyclopenten-1- yl}octanoic acid (3)	Hydrogen bond	ASN 180, ALA 182, LEU 181, THR 241	-7.7
		Hydrophobic bond	HIS 218, VAL 215, TYR 240	
		Van der Waals	GLY 179, TYR 210, SER 239, GLU 219, TYR 237, PRO 238, ARG 214, LEU 235	
	(R, Z)-N-(1-hydroxy-3-phenylpropan-2-yl)benzimidic acid (4)	Hydrogen bond	TYR 237, SER 239, UNK 1	-7.5
		Hydrophobic bond	HIS 218, VAL 215	
		Van der Waals	HIS 222, GLU 219, HIS 228, PRO 238, TYR 240, LEU 235, THR 241, ARG 214, LEU 181, ALA 182, ASN 180	
	7-Methyl-3-methylene-6-(3-oxobutyl)-3,3a,4,7,8,8a-hexahydro-2H-cyclohepta[b] furan-2-one (5)	Hydrogen bond	LEU 181, ASN 180, ALA 182	-7.4
		Hydrophobic bond	HIS 218, VAL 215	
		Van der Waals	ARG 214, THR 241, SER 239, TYR 240, LEU 235, TYR 237, GLU 219, GLY 179, PRO 238	
	1a,5,7a-trimethyl-1a,6a,7a,8,9,9a-hexahedrons(oxireno) [2',3':4,5;2",3":8,9]cyclodeca[1,2-b] furan-6(2H)-one (6)	Hydrogen bond	TYR 237, ASN 180, VAL 215	-7.3
		Hydrophobic bond	HIS 218, LEU 181, HIS 228, PRO 238	
		Van der Waals	SER 239, TYR 240, GLY 179, ALA 182, GLU 219	
	12-Oxo phytodienoic acid (7)	Hydrogen bond	THR 241, ASN 180	-7.2
		Hydrophobic bond	VAL 215, HIS 218, LEU 181, TYR 240	
		Van der Waals	ARG 214, LEU 235, SER 239, ALA 234, TYR 237, TYR 210, GLY 179, ALA 182, GLU 219	
	Curcolonol (8)	Hydrogen bond	ALA 182, ASN 180, TYR 240, SER 239	-7.2
		Hydrophobic bond	LEU 181, VAL 215, PRO 238, HIS 218	
		Van der Waals	GLU 219, TYR 237	
	5-(7-hydroxy-6-methyloctyl) furan-2(5H)-one (9)	Hydrogen bond	ALA 182, THR 241	-7.2
		Hydrophobic bond	LEU 181, VAL 215, HIS 218	
		Van der Waals	GLY 179, ASN 180, TYR 237, LEU 235, SER 239, TYR 240, ARG 214, GLU 219, PRO 238	

Extract Type	Compound (Compound number)	Bond interaction	Amino acid residue	Bond energy (kcal/mol)
ACS 70	Trans-3-indoleacrylic acid (1)	Hydrogen bond	TYR 237, ALA 182	-8.0
		Hydrophobic bond	VAL 215, HIS 218, SER 239	
		Van der Waals	LEU 235, THR 241, ARG 214, TYR 240, LEU 181, GLY 179, ASN 180, PRO 238	
	6-(2-hydroxy-4-phenylbutyl)-4-methoxypyran-2-one (2)	Hydrogen bond	ALA 182, ASN 180, HIS 183	-7.8
		Hydrophobic bond	HIS 218, SER 239, HIS 228, VAL 215	
		Van der Waals	TYR 237, LEU 235, THR 241, ARG 214, TYR 240, LEU 181, ALA 184, GLU 219, HIS 222	
	8-{3-Oxo-2-[(2E)-2-penten-1-yl]-1-cyclopenten-1- yl}octanoic acid (3)	Hydrogen bond	ASN 180, ALA 182, LEU 181, THR 241	-7.7
		Hydrophobic bond	HIS 218, VAL 215, TYR 240	
		Van der Waals	GLY 179, TYR 210, SER 239, GLU 219, TYR 237, PRO 238, ARG 214, LEU 235	
	(R, Z)-N-(1-hydroxy-3-phenylpropan-2-yl)benzimidic acid (4)	Hydrogen bond	TYR 237, SER 239, UNK 1	-7.5
		Hydrophobic bond	HIS 218, VAL 215	
		Van der Waals	HIS 222, GLU 219, HIS 228, PRO 238, TYR 240, LEU 235, THR 241, ARG 214, LEU 181, ALA 182, ASN 180	
	4-(5,6-dihydroxyheptyl)-3-methylfuran-2(5H)-one (18)	Hydrogen bond	THR 241, LEU 235, TYR 237, ALA 182, LEU 181	-7.4
		Hydrophobic bond	ARG 214, VAL 215, HIS 218	
		Van der Waals	SER 239, TYR 240, GLU 219, ASN 180	
	12-Oxo phytodienoic acid (7)	Hydrogen bond	THR 241, ASN 180	-7.2
		Hydrophobic bond	VAL 215, HIS 218, LEU 181, TYR 240	
		Van der Waals	ARG 214, LEU 235, SER 239, ALA 234, TYR 237, TYR 210, GLY 179, ALA 182, GLU 219	
	19-Norandrostenedione (19)	Hydrophobic bond	HIS 218, VAL 215, LEU 181	-7.2
		Van der Waals	ALA 182, ASN 180, HIS 228, PRO 238, SER 239, TYR 237, LEU 235, THR 241, ARG 214, TYR 240	
	Vitexin (20)	Hydrogen bond	SER 239	-7.2
		Hydrophobic bond	VAL 215, HIS 218, HIS 228	
		Van der Waals	GLU 219, HIS 183, ALA 182, TYR 237, THR 241, ARG 214, PRO 238, ASN 180, TYR 240, GLY 179, LEU 181	
	9S,13R-12-Oxophytodienoic Acid (21)	Hydrogen bond	THR 241, LEU 235, LEU, 181, ASN 180, ALA 182	-7.1
		Hydrophobic bond	VAL 215, HIS 218, HIS 228	
		Van der Waals	ARG 214, TYR 240, SER 239, TYR 237, ALA 234, PRO 238, GLU 219	
	7-(2-aminophenyl)heptanoic Acid (22)	Hydrogen bond	HIS 218, TYR 240	-7.0
		Hydrophobic bond	ARG 214, LEU 181, ALA 182, VAL 215	
		Van der Waals	GLU 219, THR 241, LEU 235, TYR 237, PRO 238, SER 239	
ACS 50	6-(2-hydroxy-4-phenylbutyl)-4-methoxypyran-2-one (2)	Hydrogen bond	ALA 182, ASN 180, HIS 183	-7.8
		Hydrophobic bond	HIS 218, SER 239, HIS 228, VAL 215	
		Van der Waals	TYR 237, LEU 235, THR 241, ARG 214, TYR 240, LEU 181, ALA 184, GLU 219, HIS 222	
	(R, Z)-N-(1-hydroxy-3-phenylpropan-2-yl)benzimidic acid (4)	Hydrogen bond	TYR 237, SER 239, UNK 1	-7.5
		Hydrophobic bond	HIS 218, VAL 215	
		Van der Waals	HIS 222, GLU 219, HIS 228, PRO 238, TYR 240, LEU 235, THR 241, ARG 214, LEU 181, ALA 182, ASN 180	
	4-(5,6-dihydroxyheptyl)-3-methylfuran-2(5H)-one (18)	Hydrogen bond	THR 241, LEU 235, TYR 237, ALA 182, LEU 181	-7.4
		Hydrophobic bond	ARG 214, VAL 215, HIS 218	
		Van der Waals	SER 239, TYR 240, GLU 219, ASN 180	
	12-Oxo phytodienoic acid (7)	Hydrogen bond	THR 241, ASN 180	-7.2
		Hydrophobic bond	VAL 215, HIS 218, LEU 181, TYR 240	
		Van der Waals	ARG 214, LEU 235, SER 239, ALA 234, TYR 237, TYR 210, GLY 179, ALA 182, GLU 219	
	19-Norandrostenedione (19)	Hydrophobic bond	HIS 218, VAL 215, LEU 181	-7.2
		Van der Waals	ALA 182, ASN 180, HIS 228, PRO 238, SER 239, TYR 237, LEU 235, THR 241, ARG 214, TYR 240	
	Vitexin (20)	Hydrogen bond	SER 239	-7.2
		Hydrophobic bond	VAL 215, HIS 218, HIS 228	
		Van der Waals	GLU 219, HIS 183, ALA 182, TYR 237, THR 241, ARG 214, PRO 238, ASN 180, TYR 240, GLY 179, LEU 181	

Extract Type	Compound (Compound number)	Bond interaction	Amino acid residue	Bond energy (kcal/mol)
ACS 50	9S,13R-12-Oxophytodienoic Acid (21)	Hydrogen bond	THR 241, LEU 235, LEU 181, ASN 180, ALA 182	-7.1
		Hydrophobic bond	VAL 215, HIS 218, HIS 228	
		Van der Waals	ARG 214, TYR 240, SER 239, TYR 237, ALA 234, PRO 238, GLU 219	
	Jasmonic acid (28)	Hydrogen bond	ALA 182, GLU 219, TYR 237	-7.0
		Van der Waals	THR 241, VAL 215, TYR 240, LEU 181, HIS 183, HIS 218, PRO 238, SER 239, ARG 214, LEU 235	
	4-Coumaric acid (29)	Hydrogen bond	THR 241, TYR 240	-6.9
		Hydrophobic bond	VAL 215, ALA 182, LEU 181	
		Van der Waals	LEU 235, HIS 218, ASN 180, GLU 219, ARG 214	
	Corchorifatty acid F (30)	Hydrogen bond	THR 241, SER 239, TYR 237	-6.8
		Hydrophobic bond	TYR 240, ARG 214, HIS 218, VAL 215	
		Van der Waals	PRO 238, GLY 179, ASN 180, ALA 182, HIS 228, LEU 181, LEU 235, ALA 234	
ACS EA	6-(2-hydroxy-4-phenylbutyl)-4-methoxypyran-2-one (2)	Hydrogen bond	ALA 182, ASN 180, HIS 183	-7.8
		Hydrophobic bond	HIS 218, SER 239, HIS 228, VAL 215	
		Van der Waals	TYR 237, LEU 235, THR 241, ARG 214, TYR 240, LEU 181, ALA 184, GLU 219, HIS 222	
	8-{3-Oxo-2-[(2E)-2-penten-1-yl]-1-cyclopenten-1-yl}octanoic acid (3)	Hydrogen bond	ASN 180, ALA 182, LEU 181, THR 241	-7.7
		Hydrophobic bond	HIS 218, VAL 215, TYR 240	
		Van der Waals	GLY 179, TYR 210, SER 239, GLU 219, TYR 237, PRO 238, ARG 214, LEU 235	
	(R, Z)-N-(1-hydroxy-3-phenylpropan-2-yl)benzimidic acid (4)	Hydrogen bond	TYR 237, SER 239, UNK 1	-7.5
		Hydrophobic bond	HIS 218, VAL 215	
		Van der Waals	HIS 222, GLU 219, HIS 228, PRO 238, TYR 240, LEU 235, THR 241, ARG 214, LEU 181, ALA 182, ASN 180	
	(9cis)-Retinal (32)	Hydrogen bond	THR 241	-7.2
		Hydrophobic bond	TYR 240, ARG 214, HIS 218, VAL 215, ALA 182, LEU 181, PRO 238, HIS 228	
		Van der Waals	GLY 179, ASN 180, SER 239, LEU 235, TYR 237, GLU 219	
	12-Oxo phytodienoic acid (7)	Hydrogen bond	THR 241, ASN 180	-7.2
		Hydrophobic bond	VAL 215, HIS 218, LEU 181, TYR 240	
		Van der Waals	ARG 214, LEU 235, SER 239, ALA 234, TYR 237, TYR 210, GLY 179, ALA 182, GLU 219	
	19-Norandrostenedione (19)	Hydrophobic bond	HIS 218, VAL 215, LEU 181	-7.2
		Van der Waals	ALA 182, ASN 180, HIS 228, PRO 238, SER 239, TYR 237, LEU 235, THR 241, ARG 214, TYR 240	
	9S,13R-12-Oxophytodienoic Acid (21)	Hydrogen bond	THR 241, LEU 235, LEU 181, ASN 180, ALA 182	-7.1
		Hydrophobic bond	VAL 215, HIS 218, HIS 228	
		Van der Waals	ARG 214, TYR 240, SER 239, TYR 237, ALA 234, PRO 238, GLU 219	
	Corchorifatty acid F (30)	Hydrogen bond	THR 241, SER 239, TYR 237	-6.8
		Hydrophobic bond	TYR 240, ARG 214, HIS 218, VAL 215	
		Van der Waals	PRO 238, GLY 179, ASN 180, ALA 182, HIS 228, LEU 181, LEU 235, ALA 234	
			MMP12	
Native ligand	Acetohydroxamic acid (LN12)	Hydrogen bond	ALA 182, HIS 222, HIS 218, HIS 228, GLU 219	-3.4
		Van der Waals	PRO 238, LEU 181, ILE 180, HIS 183	
ACS 96	L(-)-2-Amino-3-phenyl-1-propanol (10)	Hydrogen bond	ALA 182, GLU 219	-4.0
		Hydrophobic bond	ILE 180	
		Van der Waals	HIS 228, PRO 238, LEU 181, HIS 218, HIS 222, HIS 183, ALA 184	
	L-Phenylalanine (11)	Hydrogen bond	ALA 182, GLU 219, HIS 228, HIS 218	-4.0
		Hydrophobic bond	ILE 180	
		Van der Waals	LEU 181, HIS 183, ALA 184, HIS 222, PRO 234	
	Nicotinic acid (12)	Hydrogen bond	HIS 218, HIS 228, UNK 1	-4.0
		Hydrophobic bond	ILE 180	
		Van der Waals	HIS 183, ALA 182, GLU 219, LEU 181, PRO 238, HIS 222	
	4-Phenylbutyric acid (13)	Hydrogen bond	ALA 182, HIS 228, HIS 222, HIS 218	-3.8
		Hydrophobic bond	ILE 180	
		Van der Waals	PRO 238, LEU 181, GLU 219, HIS 183	

Extract Type	Compound (Compound number)	Bond interaction	Amino acid residue	Bond energy (kcal/mol)
ACS 96	Azelaic acid (14)	Hydrogen bond	HIS 222, HIS 228, HIS 218, ALA 182, GLU 219, ALA 184	-3.7
		Hydrophobic bond	ILE 180	
		Van der Waals	PRO 238, HIS 183	
	Phthaldialdehyde (15)	Hydrogen bond	HIS 222, HIS 218, HIS 228	-3.6
		Hydrophobic bond	ILE 180, HIS 183	
		Van der Waals	ALA 182, GLU 219	
	6-Pentyl-2H-pyran-2-one (16)	Hydrogen bond	HIS 228	-3.1
		Hydrophobic bond	HIS 218	
		Van der Waals	GLU 219, LEU 181, HIS 222, ALA 182, PRO 238, ILE 180, HIS 183	
	Jasmone (17)	Hydrophobic bond	PRO 238, HIS 228	-2.9
		Van der Waals	HIS 218, GLU 219, ALA 182, HIS 222, ALA 184, HIS 183, ILE 180	
ACS 70	Gluconic acid (23)	Hydrogen bond	HIS 218, ALA 182, PRO 238, HIS 228, HIS 222	-4.3
		Van der Waals	THR 215, GLU 219, ILE 180, HIS 183, ALA 184, LEU 181	
	L(-)-2-Amino-3-phenyl-1-propanol (10)	Hydrogen bond	ALA 182, GLU 219	-4.0
		Hydrophobic bond	ILE 180	
		Van der Waals	HIS 228, PRO 238, LEU 181, HIS 218, HIS 222, HIS 183, ALA 184	
	L-Phenylalanine (11)	Hydrogen bond	ALA 182, GLU 219, HIS 228, HIS 218	-4.0
		Hydrophobic bond	ILE 180	
		Van der Waals	LEU 181, HIS 183, ALA 184, HIS 222, PRO 234	
	Nicotinic acid (12)	Hydrogen bond	HIS 218, HIS 228, UNK 1	-4.0
		Hydrophobic bond	ILE 180	
		Van der Waals	HIS 183, ALA 182, GLU 219, LEU 181, PRO 238, HIS 222	
	Uracil (24)	Hydrogen bond	GLU 219	-3.9
		Electrostatic bond	HIS 218, HIS 228	
		Van der Waals	ILE 180, PRO 238, ALA 182, HIS 222, ALA 184, HIS 183	
	2,4-Dimethylbenzaldehyde (25)	Hydrogen bond	HIS 218	-3.8
		Hydrophobic bond	ILE 180, HIS 228	
		Van der Waals	ALA 184, HIS 183, HIS 222, ALA 182, PRO 238, GLU 219	
	4-Phenylbutyric acid (13)	Hydrogen bond	THR 241, SER 239, LEU 235	-3.8
		Hydrophobic bond	HIS 218, VAL 215	
		Van der Waals	TYR 237, TYR 240, ARG 214, LEU 181, PRO 238	
	Guanine (26)	Hydrogen bond	GLU 219, ALA 184, ALA 182, UNK 1	-3.8
		Electrostatic bond	HIS 228	
		Van der Waals	HIS 218, HIS 222, HIS 183, ILE 180, LEU 181	
	Azelaic acid (14)	Hydrogen bond	HIS 222, HIS 228, HIS 218, ALA 182, GLU 219, ALA 184	-3.7
		Hydrophobic bond	ILE 180	
		Van der Waals	PRO 238, HIS 183	
	Hypoxanthine (27)	Hydrogen bond	UNK 1	-3.7
		Hydrophobic bond	HIS 218, HIS 222	
		Electronic bond	HIS 228	
		Van der Waals	GLU 219, ALA 182, ALA 184, HIS 183, ILE 180, PRO 238	
ACS 50	Gluconic acid (23)	Hydrogen bond	HIS 218, ALA 182, PRO 238, HIS 228, HIS 222	-4.3
		Van der Waals	THR 215, GLU 219, ILE 180, HIS 183, ALA 184, LEU 181	
	Nicotinic acid (12)	Hydrogen bond	HIS 218, HIS 228, UNK 1	-4.0
		Hydrophobic bond	ILE 180	
		Van der Waals	HIS 183, ALA 182, GLU 219, LEU 181, PRO 238, HIS 222	
	Uracil (24)	Hydrogen bond	GLU 219	-3.9
		Electrostatic bond	HIS 218, HIS 228	
		Van der Waals	ILE 180, PRO 238, ALA 182, HIS 222, ALA 184, HIS 183	

Extract Type	Compound (Compound number)	Bond interaction	Amino acid residue	Bond energy (kcal/mol)
ACS 50	Guanine (26)	Hydrogen bond	GLU 219, ALA 184, ALA 182, UNK 1	-3.8
		Electrostatic bond	HIS 228	
		Van der Waals	HIS 218, HIS 222, HIS 183, ILE 180, LEU 181	
	Azelaic acid (14)	Hydrogen bond	HIS 222, HIS 228, HIS 218, ALA 182, GLU 219, ALA 184	-3.7
		Hydrophobic bond	ILE 180	
		Van der Waals	PRO 238, HIS 183	
	Hypoxanthine (27)	Hydrogen bond	UNK 1	-3.7
		Hydrophobic bond	HIS 218, HIS 222	
		Electronic bond	HIS 228	
		Van der Waals	GLU 219, ALA 182, ALA 184, HIS 183, ILE 180, PRO 238	
	Phthaldialdehyde (15)	Hydrogen bond	HIS 222, HIS 218, HIS 228	-3.6
		Hydrophobic bond	ILE 180, HIS 183	
		Van der Waals	ALA 182, GLU 219	
	Citric acid (31)	Hydrogen bond	HIS 218, ALA 182, HIS 222	-2.8
		Van der Waals	HIS 183, ILE 180, ALA 184, LEU 181, GLU 219, HIS 228, PRO 238	
	Jasmonic acid (28)	Hydrogen bond	GLU 219	-1.9
		Van der Waals	LEU 181, PRO 238, HIS 218, ALA 182, ILE 180, HIS 228, HIS 222, HIS 183, ALA 184, THR 215	
ACS EA	2,4-Dimethylbenzaldehyde (25)	Hydrogen bond	HIS 218	-3.8
		Hydrophobic bond	ILE 180, HIS 228	
		Van der Waals	ALA 184, HIS 183, HIS 222, ALA 182, PRO 238, GLU 219	
	4-Phenylbutyric acid (13)	Hydrogen bond	THR 241, SER 239, LEU 235	-3.8
		Hydrophobic bond	HIS 218, VAL 215	
		Van der Waals	TYR 237, TYR 240, ARG 214, LEU 181, PRO 238	
	Phthaldialdehyde (15)	Hydrogen bond	HIS 222, HIS 218, HIS 228	-3.6
		Hydrophobic bond	ILE 180, HIS 183	
		Van der Waals	ALA 182, GLU 219	
	6-Pentyl-2H-pyran-2-one (16)	Hydrogen bond	HIS 228	-3.1
		Hydrophobic bond	HIS 218	
		Van der Waals	GLU 219, LEU 181, HIS 222, ALA 182, PRO 238, ILE 180, HIS 183	
	(R, Z)-N-(1-hydroxy-3-phenylpropan-2-yl)acetamide acid (33)	Hydrogen bond	ALA 182, UNK 1, HIS 222, HIS 218	-1.8
		Hydrophobic bond	HIS 218	
		Van der Waals	LEU 181, PRO 238, GLU 219, HIS 228, HIS 183, ALA 184, ILE 180	

In contrast, the trans-3-indoleacrylic acid compound formed two hydrogen bonds with ALA 182 and TYR 237 and established strong hydrophobic bonds with HIS 218 and SER 239 (Fig. 2). Hydrophobic interactions between the protein side chains and ligands play a significant role in free energy binding, as hydrophobic groups repel water and other polar groups while attracting nonpolar ligand groups (Bronowska 2011). There is a similarity in the amino acid residues involved in the molecular interactions between the test ligand and the native ligand. Specifically, the amino acid residues ALA 182, ASN 180, and LEU 181 are present in the molecular interactions between the native ligand and the test ligand with the receptor. This similarity in amino acid residues suggests that the test ligand may exhibit competitive inhibition (Williams et al. 2012; Gaspersz and Sohilait 2019).

Meanwhile, on MMP12, the average ACS extract compounds from each solvent variation had higher scores than acetohydroxamic acid, as shown in Table 2. This indicates that the ACS extract compounds likely exhibit superior

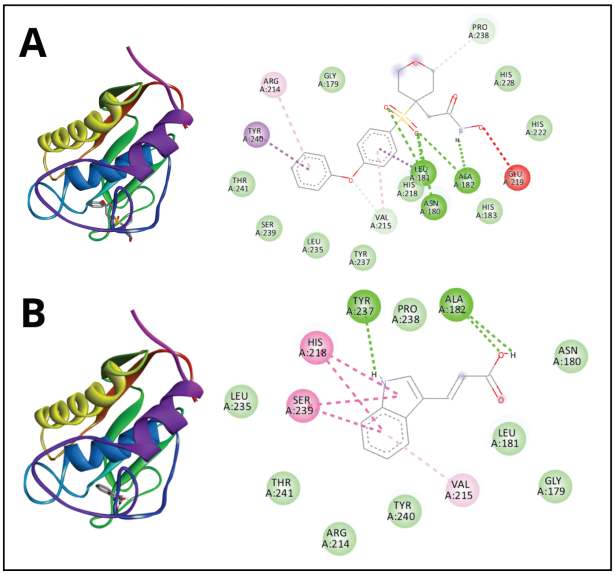

Figure 2. Molecular interaction of (**A**) LN1 (**B**) trans-3-indoleacrylic acid.

inhibitory activity against MMP12 compared to acetohydroxamic acid. Among them, gluconic acid (with a binding energy of -4.3 kcal/mol) found in ACS 70 and ACS 50 extracts demonstrated the lowest binding affinity for MMP12. Gluconic acid interacts with ALA 182, HIS 218, HIS 228, PRO 238, and HIS 222 (Fig. 3). Previous research (Arda et al. 2024) showed the potential of propolis against MMP12, where the pinostrobin compound interacted with ALA 182 and showed excellent binding affinity for MMP12.

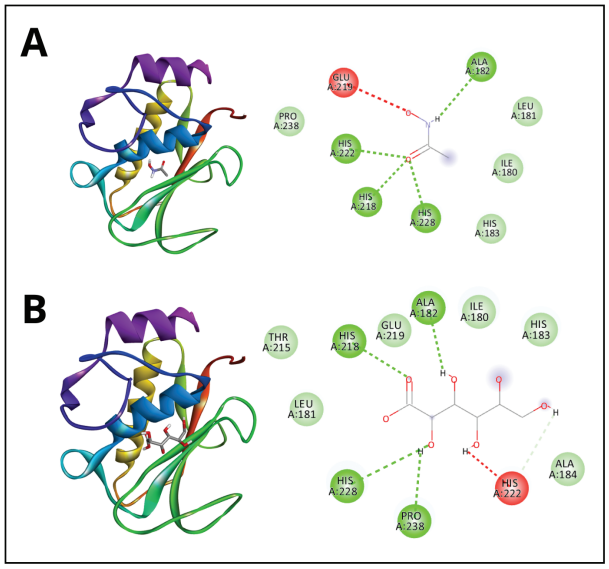

Figure 3. Molecular interaction of (**A**) LN12 (**B**) gluconic acid.

In vitro analysis of NIH-3T3 cell proliferation

Prior to conducting the proliferation assay of the extract on NIH-3T3 cells, we assessed cell viability using MTT methods to determine the non-toxic concentration of the extracts. At a concentration of 25 mg/L, the order of increased cell viability for the ACS extracts across various concentration variations was ACS 96 > ACS 50 > ACS 70 > ACS EA. At higher concentrations of 100, 200, and 400 µg/mL, the increase order shifted to ACS 96 > ACS EA > ACS 70 > ACS 50. For any sample designated as biocompatible, the percent cell viability should be at least 70% or higher (Bokhari et al. 2024). As shown in Fig. 4, the average cell viability for each solvent and concentration variation remained above 70%, indicating that the extracts did not harm NIH-3T3 fibroblast cells. In line with previous studies (Hanafiah et al. 2019; Sugiaman et al. 2024), ACS extract in 70% ethanol maintained cell viability above 70%. The presence of bioactive compounds in ACS extract promotes cell growth and increases cell survival. Fig. 4 also shows that the 25, 50, 100, 200, and 400 µg/mL ACS leaf extract concentrations are not significant to the cell control, suggesting that the extracts are safe for conducting proliferation tests on NIH-3T3 fibroblast cells. However, to prevent overdose that would induce necrosis of NIH-3T3 fibroblast cells, it is assumed that a concentration of 200 µg/mL is within safe limits.

As depicted in Fig. 5A, NIH-3T3 cell proliferation significantly increased following treatment with ACS 70

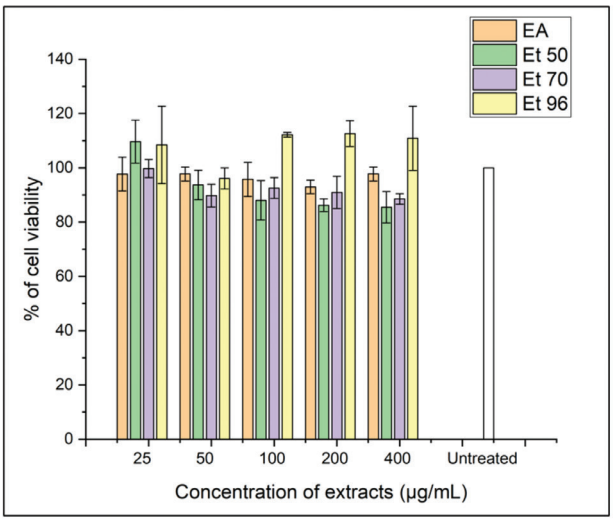

Figure 4. Cell viability of NIH-3T3 fibroblasts treated with *Anredera cordifolia* (Ten.) Steenis extract. Cells were treated with extracts for 24 hours, and an MTT assay was performed to determine the viability of the cells. Untreated control was set at 100%; (a) indicates a significant difference at $p < 0.05$.

at concentrations ranging from 8 µg/mL to 200 µg/mL during a 24-hour incubation period, compared to untreated cells. Similarly, ACS 96% induced cell proliferation starting from 2 µg/mL up to 40 µg/mL relative to control cells, while no significant proliferation was observed when cells were treated with ACS 50 and ACS EA up to a concentration of 200 µg/mL for 24 hours.

The effect of ACS extracts on NIH-3T3 cell proliferation was also examined at 48 hours of incubation. As shown in Fig. 5B, NIH-3T3 cells treated with ACS EA exhibited a significant decrease in proliferation at concentrations ranging from 2 µg/mL to 8 µg/mL. ACS 96 and ACS 70 also decreased starting from 8 µg/mL, while ACS 50 remained relatively stable.

Fig. 5C shows a decrease in NIH-3T3 cell proliferation after 72 hours of treatment with ACS extracts. However, the average cell viability is still above 70% in each variation, which is still considered a safe limit. Cell viability of ACS EA extract at a concentration of 2 µg/mL decreased as the concentration increased. Similarly, ACS 96 and ACS 50 extracts showed a decline in cell viability with increasing concentrations. Conversely, the ACS 70 extract maintained more stable cell viability, particularly at a 200 µg/mL concentration, compared to the other extract variations.

Conclusion

Thirty-three (33) bioactive compounds were positively identified in ACS extract using UHPLC-HRMS. This study successfully used a computational screening strategy to find potential wound-healing agents in ACS by inhibiting collagenase (MMP1) and elastase (MMP12). 16 compounds exhibited the lowest affinity values for MMP1, 15 had the lowest affinity values for MMP12, and the remaining 2 compounds showed low affinity for both MMP1 and

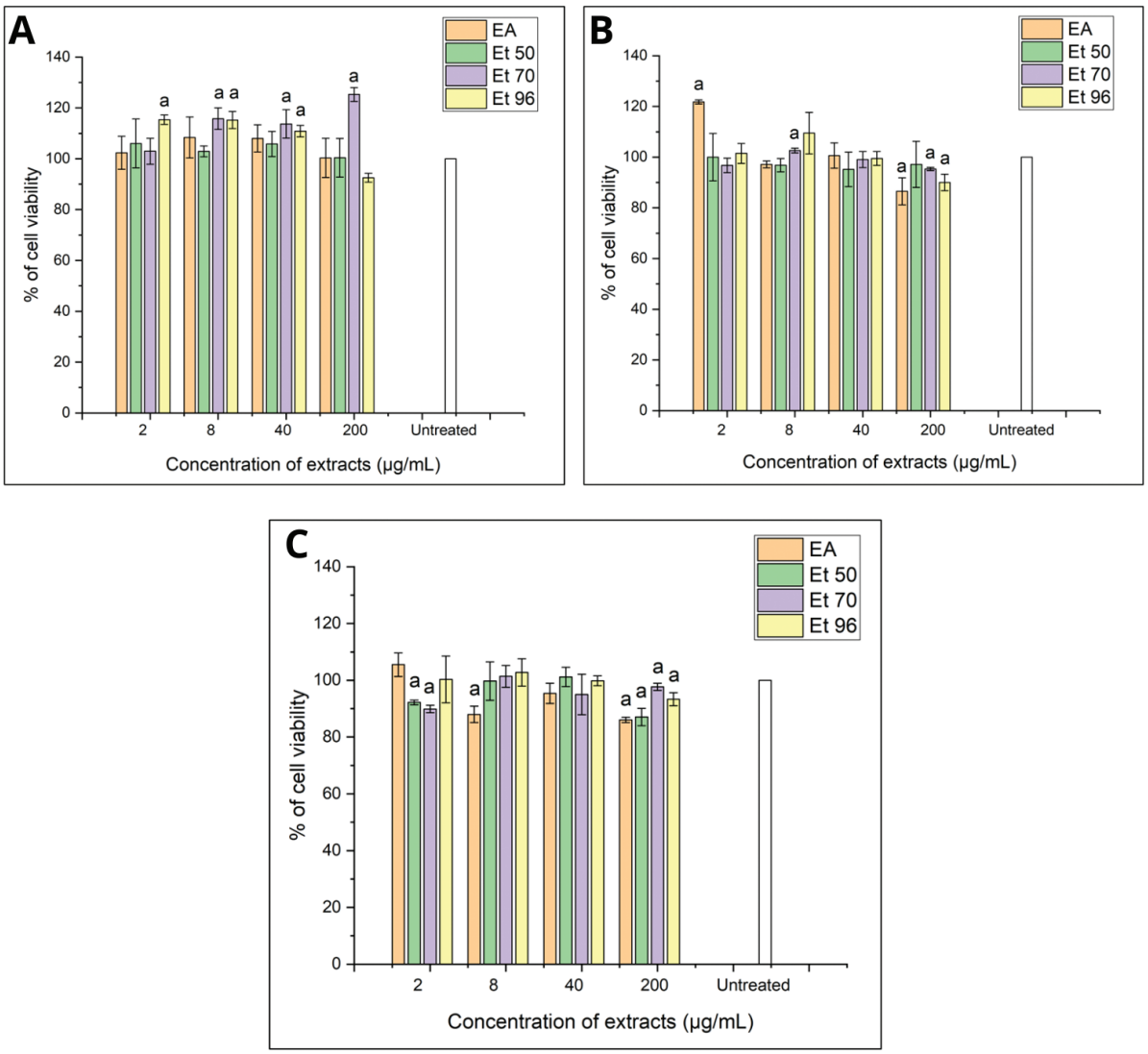

Figure 5. Proliferation of NIH-3T3 cells treated with ACS EA, ACS 50, ACS 70, and ACS 96 extracts for 24 hours (**A**), 48 hours (**B**), and 72 hours (**C**). Cell proliferation values are presented as SD of three independent experiments. Untreated control was set at 100%; (a) indicates a significant difference at $p < 0.05$.

MMP12. MMP1 is a collagenase, and MMP12 is an elastase inhibitor, as demonstrated by in silico assay. Trans-3-indole acrylic acid is a collagenase, and gluconic acid is an elastase inhibitor, as demonstrated by in silico assay. These compounds were detected in the ACS extract 70. Furthermore, in vitro testing of ACS 70 extract showed the highest proliferation activity of NIH-3T3 fibroblast cells compared to other extracts. ACS 70 extract is potentially an active ingredient for wound healing, but it still needs an *in vitro* cell migration assay and *in vivo* tests on animals.

Additional information

Conflict of interest

The authors have declared that no competing interests exist.

Ethical statements

The authors declared that no clinical trials were used in the present study.

The authors declared that no experiments on humans or human tissues were performed for the present study.

The authors declared that no informed consent was obtained from the humans, donors or donors' representatives participating in the study.

The authors declared that no experiments on animals were performed for the present study.

Use of commercially available immortalised human and animal cell lines: We used NIH-3T3/Swiss mouse embryos obtained from the Food and Science Technology Department of National Pingtung Science Technology (NPUST, Pingtung, Taiwan).

Funding

The authors gratefully acknowledge the financial support for this project, provided by the Health Research Organization – National Agency for Research and Innovation (BRIN) Indonesia and Faculty of Science and Mathematics of Universitas Diponegoro Semarang Indonesia.

Author contributions

All authors contributed significantly to this manuscript, participated in the research, wrote, reviewed/edited, and approved the final draft for publication.

Author ORCIDs

Khairunnisa Aulia Dewi https://orcid.org/0009-0004-5726-0265
Susi Kusumaningrum https://orcid.org/0000-0002-5388-6285
Nor Basid Adiwibawa Prasetya https://orcid.org/0000-0002-6956-3667
Siska Andrina Kusumastuti https://orcid.org/0000-0002-6270-3356
Eriawan Rismana https://orcid.org/0000-0002-7601-0673
Ngatinem Ngatinem https://orcid.org/0000-0003-4811-3541
Nuralih Nuralih https://orcid.org/0000-0001-9145-2093
Mayriska Tri Wulansari https://orcid.org/0009-0002-0761-9714

Data availability

All of the data that support the findings of this study are available in the main text or Supplementary Information.

References

Agustini K, Sangande F, Nuralih N, Harahap AM, Ningsih S, Bahtiar A (2024) Molecular mechanism elucidation of *Ocimum basilicum* as anticancer using system bioinformatic approach supported by in vitro assay. Pharmacia 71: 1–12. https://doi.org/10.3897/pharmacia.71.e127395

Alba TM, de Pelegrin CMG, Sobottka AM (2020) Pharmacognosy ethnobotany, ecology, pharmacology, and chemistry of *Anredera cordifolia* (Basellaceae): a review. Rodriguésia 71. https://doi.org/10.1590/2175-7860202071060

Anggraeni D, Airin CM, Raharjo S (2017) The effectiveness of ethanol extract of binahong leaves on diabetic wound healing. Indonesian Journal of Veterinary Sciences 11(4). https://doi.org/10.21157/j.ked.hewan.v11i4.6562

Arda AG, Syaifie PH, Ramadhan D, Jauhar MM, Nugroho DW, Kaswati NMN, Noviyanto A, Safihtri M, Rochman NT, Andrianto D, Mardliyati E (2024) Activity of propolis compounds as potential MMP1 and MMP2 inhibitors by in silico studies in wound healing application. Journal of Pharmacy & Pharmacognosy Research 12: 264–285. https://doi.org/10.56499/jppres23.1719_12.2.264

Astuti SM, Sakinah MA, Andayani RB, Risch A (2011) Determination of saponin compound from *Anredera cordifolia* (Ten) Steenis plant (binahong) to potential treatment for several diseases. Journal of Agricultural Science 3: 224. https://doi.org/10.5539/jas.v3n4p224

Bari IN, Kato-Noguchi H, Iwasaki A, Suenaga K (2019) Allelopathic potency and an active substance from *Anredera cordifolia* (Tenore) Steenis. Plants 8: 134. https://doi.org/10.3390/plants8050134

Bokhari N, Ali A, Yasmeen A, Khan R, Haider S, Sharif F (2024) Fabrication of bioactive silk composite meshes for hernia repair and guided soft tissue remodeling: In silico, in vitro and in vivo models. Applied Materials Today 38: 102261. https://doi.org/10.1016/j.apmt.2024.102261

Bronowska AK (2011) Thermodynamics of ligand-protein interactions: implications for molecular design. In: Moreno-Pirajan JC (Ed.) Thermodynamics-Interaction Studies-Solids, Liquids and Gases. IntechOpen. https://doi.org./10.5772/19447

Fachriyah E, Ayu T, Kusrini D (2019) Identification of Phenolic acid from ethanol extract leaves binahong (*Anredera cordifolia* (ten) stennis) and antioxidant activity test. Journal of Physics: Conference Series 1217: 012051. https://doi.org./10.1088/1742-6596/1217/1/012051

Feriyani F, Darmawi D, Balqis U, Lubis RR (2020) The analysis of binahong leaves potential (*Anredera cordifolia*) as an alternative treatment of anticataractogenesis. Open Access Macedonian Journal of Medical Sciences 8: 820–824. https://doi.org/10.3889/oamjms.2020.4849

Gaspersz N, Sohilait MR (2019) Penambatan Molekuler α, β, dan γ-mangostin Sebagai Inhibitor α-amilase Pankreas Manusia. Indonesian Journal of Chemical Research 6: 59–66. https://doi.org/10.30598/ijcr.2019.6-nel

Hanafiah OA, Abidin T, Ilyas S, Nainggolan M, Syamsudin E (2019) Wound healing activity of binahong (*Anredera cordifolia* (Ten.) Steenis) leaves extract towards NIH-3T3 fibroblast cells. Journal of International Dental and Medical Research 12: 854–858. http://www.jidmr.com/journal/wp-content/uploads/2019/10/3-D18_735_Olivia_Afriyanti_Hanafiah.pdf

Hanafiah OA, Hanafiah DS, Dohude GA, Satria D, Livita L, Moudy NS, Rahma R (2021) Effects of 3% binahong (*Anredera cordifolia*) leaf extract gel on alveolar bone healing in post-extraction tooth socket wound in Wistar rats (*Rattus norvegicus*). F1000Research 10. https://doi.org/10.12688/f1000research.72982.2

Ke J, Ye J, Li M, Zhu Z (2021) The role of matrix metalloproteinases in endometriosis: A potential target. Biomolecules 11: 1739. https://doi.org/10.3390/biom11111739

Khoswanto C, Soehardjo I (2018) The effect of Binahong Gel (*Anredera cordifolia* (Ten.) Steenis) in accelerating the escalation expression of HIF-1α (ten). Journal of International Dental and Medical Research 11: 303–307. https://repository.unair.ac.id/114741/1/Artikel.%202.pdf

Kintoko K, Desmayanti A (2016) The effectivity of ethanolic extract of binahong leaves (*Anredera cordifolia* (tenore) steen) gel in the management of diabetic wound healing in aloxan-induced rat models. JKKI: Jurnal Kedokteran Dan Kesehatan Indonesia 227–236. https://doi.org/10.20885/JKKI.Vol7.Iss5.art9

Kostikova VA, Chernonosov AA, Kuznetsov AA, Petrova NV, Krivenko DA, Chernysheva OA, Wang W, Erst AS (2021) Identification of flavonoids in the leaves of *Eranthis longistipitata* (Ranunculaceae) by Liquid Chromatography with High-Resolution Mass Spectrometry (LC-HRMS). Plants 10: 2146. https://doi.org/10.3390/plants10102146

Leliqia NPE, Sukandar EY, Fidrianny I (2017) Antibacterial activities of *Anredera cordifolia* (Ten.) v. Steenis leaves extracts and fractions. Asian Journal of Pharmaceutical and Clinical Research 10: 10–13. https://doi.org/10.22159/ajpcr.2017.v10i12.21503

Mohammadi Z, Sharif Zak M, Majdi H, Mostafavi E, Barati M, Lotfimehr H, Ghaseminasab K, Pazoki-Toroudi H, Webster TJ, Akbarzadeh (2019) The effect of chrysin–curcumin-loaded nanofibres on the wound-healing process in male rats. Artificial Cells, Nanomedicine, and Biotechnology 47: 1642–1652. https://doi.org/10.1080/21691401.2019.1594855

Moraes LT, Trevilatto PC, Grégio AMT, De Lima AAS (2011) Quantitative Analysıs of mature and immature collagens during Oral wound healing in rats treated by Brazilian Propolis. Journal of International Dental and Medical Research 4: 106–110. http://www.jidmr.com/journal/DENTISTRY/2011/vol4_no3/1_D11-129_Antonio_Adilson_Soares_de_Lima.pdf

Mulia K, Muhammad F, Krisanti E (2017) Extraction of vitexin from binahong (*Anredera cordifolia* (Ten.) Steenis) leaves using betaine-1, 4 butanediol natural deep eutectic solvent (NADES). AIP Conference Proceedings 1823(1): 020018. https://doi.org/10.1063/1.4978091

Nissa C, Sukma GI, Madjid IJ, Sidin NM, Musyarrofah M (2022) Identifikasi Potensi Senyawa Isoflavon Dan Quercetin Dan Perbandingan Ikatan Terhadap Ace (Angiotensin-Converting Enzyme) Menggunakan Studi In Silico. Journal of Nutrition College 11: 1–5. https://doi.org/10.14710/jnc.v11i1.29500

Rehman SRu, Augustine R, Zahid AA, Ahmed R, Tariq M, Hasan A (2019) Reduced graphene oxide incorporated GelMA hydrogel promotes angiogenesis for wound healing applications. International Journal of Nanomedicine 9603–9617. https://doi.org/10.2147/IJN.S218120

Riwanti P, Izazih F, Amaliyah AJ (2020) Pengaruh perbedaan konsentrasi etanol pada kadar flavonoid total ekstrak etanol 50, 70 dan 96% Sargassum polycystum dari Madura. Journal of Pharmaceutical Care Anwar Medika 2: 82–95.

Salasanti C, Sukandar E, Fidrianny IJ (2014) Acute and sub chronic toxicity study of ethanol extract of *Anredera cordifolia* (Ten.) v. Steenis leaves. International Journal of Pharmacy and Pharmaceutical Sciences 6: 348–352. https://www.innovareacademics.in/journal/ijpps/Vol6Issue5/9335.pdf

Sugiaman VK, Pranata BMD, Susila RA, Pranata N, Rahmawati DY (2024) Antibacterial activity, cytotoxicity, and phytochemicals screenings of binahong (*Anredera cordifolia* (Ten.) steenis) leaf extract. Journal of Advanced Pharmacy Education and Research 14: 1–7. https://doi.org/10.51847/BXxQtsSl1s

Sukandar EY, Ridwan A, Sukmawan YP (2016) Vasodilation Effect of Oleanolic Acid and Apigenin as a Metabolite compound of *Anredera cordifolia* (Ten) V Steenis on isolated rabbit aortic and frog heart. International Journal of Ayurveda and Pharma Research 7: 82–84. https://doi.org/10.7897/2277-4343.075200

Wang M, Luo Y, Wang T, Wan C, Pan L, Pan S, He K, Neo A, Chen X (2021) Artificial skin perception. Advanced Materials 33: 2003014. https://doi.org/10.1002/adma.202003014

Williams LK, Li C, Withers SG, Brayer GD (2012) Order and disorder: differential structural impacts of myricetin and ethyl caffeate on human amylase, an antidiabetic target. Journal of Medicinal Chemistry 55: 10177–10186. https://doi.org/10.1021/jm301273u

Windarsih A, Warmiko HD, Indrianingsih AW, Rohman A, Ulumuddin YI (2022) Untargeted metabolomics and proteomics approach using liquid chromatography-Orbitrap high resolution mass spectrometry to detect pork adulteration in *Pangasius hypopthalmus* meat. Food Chemistry 386: 132856. https://doi.org/10.1016/j.foodchem.2022.132856

Yuliani S, Fudholi A, Pramono S, Marchaban M (2012) The effect of formula to physical properties of wound healing gel of ethanolic extract of binahong (*Anredera cordifolia* (Ten) Steenis). International Journal of Pharmaceutical Sciences and Research (IJPSR).

Yuniarti WM, Lukiswanto BS (2017) Effects of herbal ointment containing the leaf extracts of Madeira vine (*Anredera cordifolia* (Ten.) Steenis) for burn wound healing process on albino rats. Veterinary World 10: 808. https://doi.org/10.14202/vetworld.2017.808-813

Zhao X, Liang Y, Huang Y, He J, Han Y, Guo BJ (2020) Physical double- network hydrogel adhesives with rapid shape adaptability, fast self- healing, antioxidant and NIR/pH stimulus- responsiveness for multidrug- resistant bacterial infection and removable wound dressing. Advanced Functional Materials 30: 1910748. https://doi.org/10.1002/adfm.201910748

Zihlif M, Afifi F, Abu-Dahab R, Abdul Majid AMS, Somrain H, Saleh MM, Nassar ZD, Naffa R (2013) The antiangiogenic activities of ethanolic crude extracts of four *Salvia* species. BMC Complementary and Alternative Medicine 13: 1–10. https://doi.org/10.1186/1472-6882-13-358

Supplementary material 1

Determination and herbarium specimen

Authors: Susi Kusumaningrum

Data type: pdf

Link: https://doi.org/10.3897/pharmacia.72.e135811.suppl1